ELSEVIER

Journal of Alloys and Compounds 275–277 (1998) 602–605

Journal of ALLOYS AND COMPOUNDS

Magnetic properties of amorphous Sm–Co and Er–Co alloys

M.L. Soltani[a], M. Lahoubi[a], G. Fillion[b,*], B. Barbara[b]

[a]*Institut de Physique, Université d'Annaba, BP 12, El-Hadjar, 23000 Annaba, Algeria*
[b]*Laboratoire Louis Néel, CNRS-UJF, BP166, 38042 Grenoble Cedex 9, France*

Abstract

The magnetic properties have been investigated in some Sm–Co and Er–Co amorphous alloys. The samples have been obtained by r–f sputtering on different substrates. Those on glass and silica substrates have been used for structural (X-ray diffraction) and compositional (SEM) analysis. Magnetisation process (4 K$<T<$300 K) and hysteresis loops at 4 K have been studied over a wide range of fields (1 Oe$<H<$25 kOe) by using both a classical axial extraction magnetometer and a high resolution vibrating sample magnetometer (VSM). The main results are: (i) the amorphous structure is exhibited along with an enrichment of the Co element in all the deposited alloys, (ii) heat treatment and composition affect the shape of hysteresis loops, (iii) Rayleigh laws are valid but a deviation is observed in the very weak fields. © 1998 Elsevier Science S.A.

Keywords: R–Co alloys; Amorphous alloys; Hysteresis loops; Magnetisation process; Rayleigh law

1. Introduction

The amorphous rare earth-transition metal alloys, which are generally ferrimagnetic, have been intensively studied because of their potential practical applications [1–5]. They cover a wide range of saturation magnetisation, permeability, coercivity, and magnetostriction. All of these properties, and in particular the shape of hysteresis loops are dependent upon the alloy composition, heat and mechanical treatment. Amorphous films are usually prepared by sputtering or vacuum evaporation on cold crucibles.

The crystallographic structure of amorphous alloys consists of a random array of atoms with very short range correlations leading to randomly distributed local anisotropy directions. In the presence of ferromagnetic interactions, these systems are isotropic (continuous symmetry) [6]. Consequently, the magnetisation should be free from anisotropy at large scale and feature high anisotropy at short scale. Imry and Ma [7] predicted that the competition between anisotropy and exchange leads to a small-scale pattern with a correlation length scaling with $(J/D)^2$. In this paper, we attempt to relate the influence of these domains with the magnetic behaviour of several R–Co amorphous alloys, focusing especially on the Rayleigh region.

A widely used picture of domain wall pinning was given by Néel [8] in terms of random potential energy $V(x)$ of the wall position. The two main predictions of this model are: (i) the coercive field H_C is proportional to the maximal pinning force $(dV/dx)_{max}$ and (ii) the derivation of Rayleigh laws, $M=aH+bH^2$, where $bH_C/a=1$ if statistical correlations are neglected. We attempted to see whether this prediction is still valid for random anisotropy systems.

2. Experimental

2.1. Preparation of amorphous films

Rare earth-transition metal amorphous films Sm–Co and Er–Co are prepared from various targets by r–f sputtering. All the substrates were cooled at 77 K in order to prevent from crystallisation and all the films were finally given an outer coating of a few hundred angstroms of non-magnetic molybdenum protective layers. The thickness range from 0.5–1 μm for the Sm–Co films and is about 100 μm for Er–Co films. For magnetic measurement purposes, the Sm–Co samples were deposited onto Kapton 25 μm foils which permit a better filling coefficient of the sample holders. The same samples which were obtained under these same conditions on glass and silica substrates have also been used for structural (X-ray diffraction) and compositional (SEM) analysis. The Er–Co samples were deposited onto solidified vacuum grease. This last deposi-

*Corresponding author. fax: +33 4 76881191; e-mail: fillion@polycnrs-gre.fr

0925-8388/98/$19.00
PII: S0925-8388(98)00401-0

tion technique permits the handling of these films without substrate at room temperature, avoiding the strain which may come from the substrate. Heat treatments up to 750 K were carried out on these Er–Co alloys and their Curie temperature T_c was determined to be about 375 K.

2.2. Structural analysis by X-ray diffraction

The common shape of the X-ray patterns for amorphous alloys consist only of broad maxima without sharp peaks as shown in Fig. 1, except for a-$SmCo_2$ which exhibits, in addition, the pattern of crystalline Sm_2O_3, probably due to an oxidation of the target. The Scherrer formula gives an atomic correlation length of about a few interatomic distances, confirming the amorphous character of our samples.

2.3. Semi-quantitative analysis by means of SEM

Fine composition depends on vapour pressure, sputtering rate, atomic size, system geometry, sticking probabilities and sputtering coefficients. Analysis reveal a variation of the initial stoichiometry of the starting bulk material. Thus, in addition to confirmation of amorphous quality of the samples, we observed an enrichment in the Co element induced by different sticking coefficients of heavy rare earths and cobalt.

2.4. Magnetisation process and hysteresis loops

The magnetisation was measured over the temperature range from 4–300 K in magnetic fields up to 25 kOe. The hysteresis loops at 4 K have been measured by a classical axial extraction magnetometer and by a more sensitive VSM with one oersted increment in order to study the narrow Rayleigh area with a better resolution. Hysteresis loops have been performed several times and they change for each sample demagnetisation while shapes remain constant.

3. Results and discussion

We measured the magnetisation curves at 4 K for different cobalt concentrations in amorphous Sm–Co alloys. As shown in Fig. 2, the coercive field H_C decreases with increasing cobalt content. The shape of major loops corresponds to rather hard samples: (i) for a-$SmCo_8$, the loops are rectangular with $H_C=1.2$ kOe (ii) for a-$SmCo_4$, normal loop with $H_C=0.5$ kOe. For a-$SmCo_2$, it seems that the applied fields were not sufficient to generate magnetisation. In $SmCo_8$ the remanent magnetisation M_R is much larger than the one expected in an amorphous sample ($M_R=M_S/2$). In $SmCo_4$, it is slightly smaller.

The magnetisation and the coercive fields are strongly temperature dependent as shown in Fig. 3a and Fig. 3b, where the variations of M versus decreasing fields are reported for some temperatures. Sperimagnetic arrangement was confirmed in $Er_{0.25}Co_{0.75}$. Nevertheless, magnetisation measurements at 5 kOe versus temperature do not reveal a compensation temperature. The spontaneous magnetisation M_S is higher in the amorphous as-deposited film than in the heat treated film. The change of magnetisation by annealing the Er–Co amorphous alloy, under an applied field, modifies the loop, resulting in a strongly reduced loop area with a decrease of H_C from 0.6–0.4 kOe and a strong decrease in M_R.

Regarding Fig. 4, the susceptibility in strong fields shows alignment of moments in the applied field direction. In weak fields, competition between local crystalline field and exchange interactions leads to the occurrence of Imry and Ma domains of about 200±20 Å in size for amorphous

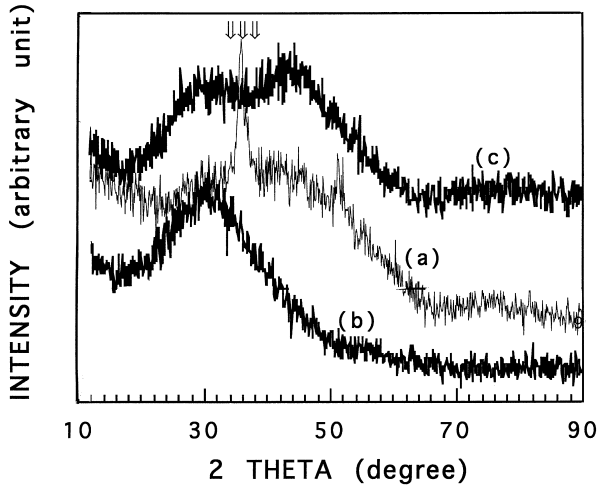

Fig. 1. X-ray diffraction patterns for: (a) as-growth a-$SmCo_2$; (b) as-grown a-$SmCo_4$; (c) as-grown $Er_{0.25}Co_{0.75}$.

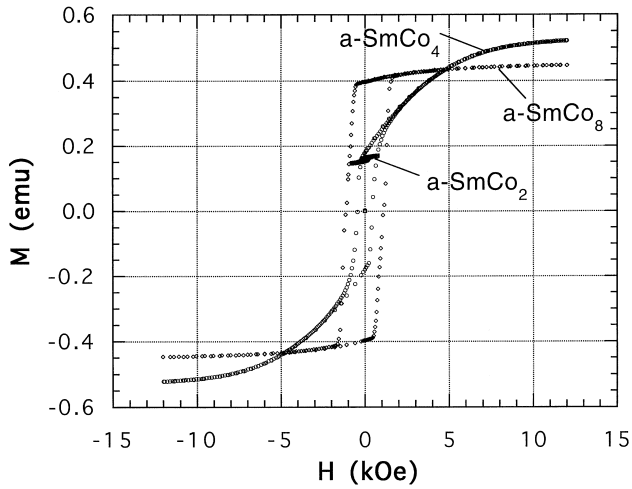

Fig. 2. Hysteresis loops at 4 K in the ±12 kOe applied field range for a-$SmCo_x$ samples.

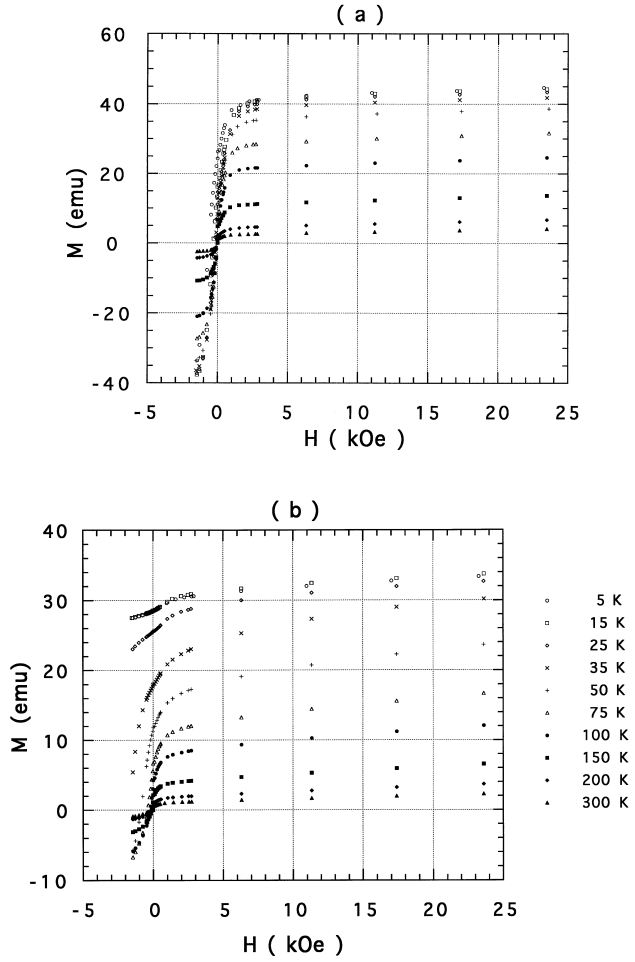

Fig. 3. Magnetisation of sputtered $ErCo_3$ versus applied field decreasing from 25 kOe at different temperatures: (a) as-grown sample; (b) annealed sample at 750 K.

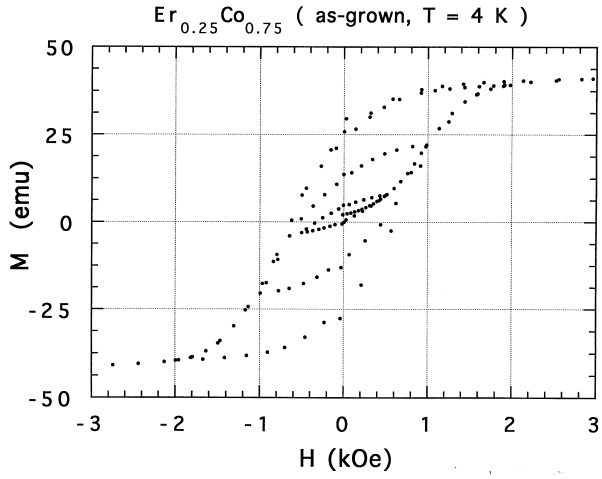

Fig. 4. Hysteresis major and minor loops at 4 K in the ±3 kOe applied field range of as-grown $Er_{0.25}Co_{0.75}$ sample.

$Er_{0.25}Co_{0.75}$ [9]. An irreversible reorganisation of these domains under an applied field is revealed in coercivity measurements.

The predictions of the Néel model can be tested by calculating the *a* and *b* Rayleigh parameters which describe respectively the reversible and the irreversible part of the hysteresis loops [10]. In order to test the Rayleigh law, we have determined the differential permeability along minor loops $\mu_r = \Delta M/\Delta H$ versus ΔH where $\Delta H = H - H_m$, H_m being defined as the peak applied field for each loop branch. After demagnetising the sample, we observed a change in *a* and *b* values by comparing several loops. Values a and b have been determined by examining μ_r along minor loops. The permeability $\mu = M_m/H_m$ versus H_m follows a Rayleigh law $\mu = a + bH_m$, although deviations have been observed by several authors [11,12]. In amorphous $Er_{0.25}Co_{0.75}$ alloy, systematic verification of the Rayleigh law has been checked in moderate H_m and $\mu(H_m)$ is accurately described by the Rayleigh law. In this case, the bH_C/a dimensionless ratio can be determined as: 2.40, 1.73 (at 10 K) and 2.80. These deduced values, which are rough estimates, relatively agree with the Néel model which does not take into account any statistical correlations. On the contrary, $\mu(H_m)$ shows a small deviation when H_m becomes smaller. In Fig. 5, the Rayleigh law was observed for $H_m > 0.30$ kOe. Below this value, a deviation appears which could be attributed either to a relatively important increase of the *b* parameter or to a change in the magnetisation versus field exponent from 2 to 3/2. Hysteresis loops measured by the VSM have allowed us to obtain Rayleigh curves around $H_C/10$ (see Fig. 6): a square root law of H_m was observed for the μ behaviour in the 100 oersted range. Nonetheless, to agree with Bertotti et al. [11,12], it should be borne in mind that the square root H_m behaviour of μ is purely empirical with no physical justification. As was suggested by Ref. [12], magnetostatic effects can partly justify the observed non-linearities. In fact, by comparing the measurements carried out on the amorphous $Er_{0.25}Co_{0.75}$ samples which present two different demagnetising factors, we observed that

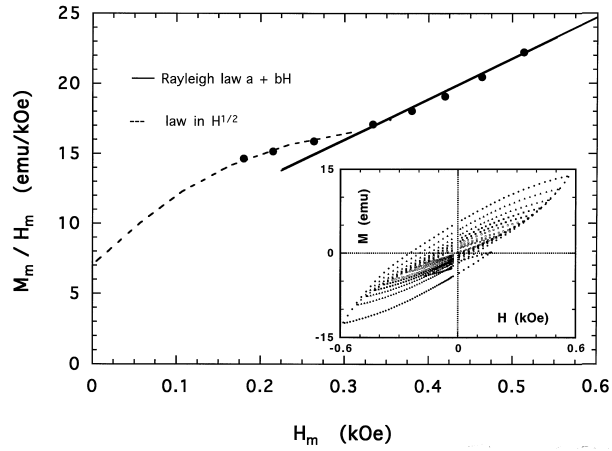

Fig. 5. Plot of $\mu = M_m/H_m$ versus peak value of applied field H_m deduced from the hysteresis loops measured with the classical axial extraction magnetometer in the ±0.4 kOe applied field range.

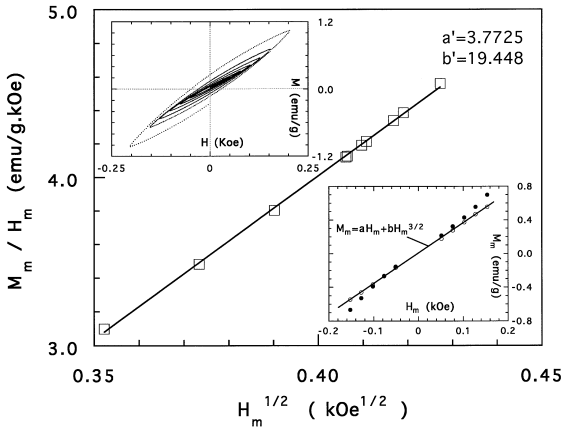

Fig. 6. Plot of $\mu = M_m/H_m$ versus square root of H_m deduced from hysteresis loops measured on only one planar piece of film with the sensitive VSM in the ± 0.2 kOe applied field range.

deviation ranges are influenced by the internal magnetostatic factor *N*.

Acknowledgements

This work was supported by a joint co-operation project ''95 MDU 343'' between the Joseph Fourier University of Grenoble (France) and Badji Mokhtar University of Annaba (Algeria).

References

[1] R. Asomoza, I.A. Campbell, H. Jouve, R. Meyer, J. Appl. Phys. 48 (1977) 3829.
[2] P. Chandhari, J.L. Cuomo, R.J. Gambino, AIP Conf. Proc. 29 (1975) 97.
[3] H. Jouve, J.P. Rebouillat, R. Meyer, IBMJ Res. Dev. 17 (1973) 66.
[4] K. Okamoto, T. Shirakawa, S. Matsushita, Y. Sakurai, IEEE Trans. Magn. MAG 10 (1974) 799.
[5] J.M. Coey, J. Chappert, J.-P. Rebouillat, T.S. Wang, Phys. Rev. Lett. 36 (1976) 1061.
[6] R. Harris, M. Plichke, M.J. Zukermann, Phys. Rev. Lett. 31 (1973) 160.
[7] Y. Imry, S.K. Ma, Phys. Rev. Lett. 35 (1975) 1399.
[8] L. Néel, Cah. Phys. 12 (1942).
[9] B. Barbara, B. Dieny, A. Lienard, J.P. Rebouillat, Solid State Commun. 55 (1985) 463–467.
[10] J.-L. Porteseil, O. Geoffroy, J. Magn. Magn. Mater. 140–144 (1995) 1855–1856.
[11] G. Bertotti, F. Fiorillo, M. Pasquale, J. Appl. Phys. 69 (1991) 5930.
[12] G. Bertotti, F. Fiorillo, M. Pasquale, J. Magn. Magn. Mater. 112 (1992) 11–13.